ELSEVIER

Journal of Nuclear Materials 307–311 (2002) 723–728

journal of nuclear materials

www.elsevier.com/locate/jnucmat

Flux dependence of deuterium retention in single crystal tungsten

M. Poon, R.G. Macaulay-Newcombe, J.W. Davis *, A.A. Haasz

Fusion Research Group, University of Toronto Institute for Aerospace Studies, 4925 Dufferin Street, Toronto, Ont., Canada M3H 5T6

Abstract

The retention of deuterium in single crystal tungsten has been measured as a function of the incident ion flux in the range of 1×10^{17}–5×10^{19} D^+/m^2 s at 300 K. Incident D_3^+ ions were implanted to fluences of 10^{21}, 10^{22}, and 10^{23} D^+/m^2 with ion energies (500 eV/D^+) below the threshold energy for elastic collision damage. Above 3×10^{18} D^+/m^2 s, little or no flux dependence is seen. However, a rapid decrease in retention is seen for incident fluxes below 10^{18} D^+/m^2 s at the 10^{21} D^+/m^2 fluence, suggesting a threshold value below which retention is strongly reduced. Flux dependence at the higher fluences show a smaller decrease in retention with decreasing flux. The observed results are consistent with trapping and trap evolution by cluster and cavity formation. The effect of specimen surface preparation has proved to be very significant, especially for the lower fluence.
© 2002 Elsevier Science B.V. All rights reserved.

1. Introduction

Tungsten's potential use as a plasma-facing material stems from its high temperature strength and high threshold for physical sputtering. However, radiative losses from tungsten impurities are very high, so the fusion process can only tolerate trace amounts of tungsten in the core plasma [1]. Although many physical and thermal properties of tungsten have been well studied and documented, the hydrogen transport and trapping properties are not nearly as well understood [2]. Hydrogen transport and trapping properties in tungsten control the tritium inventory – a major safety concern – and hydrogen recycling that may affect plasma stability.

Extensive data has been generated on the interactions of hydrogen with tungsten [2–18]. Although the results are varied and sometimes contradictory, most of the variation can be traced back to different experimental conditions or differences in the materials studied. Rather than assuming some of the data to be correct, and other data to be suspect, it is desirable to consider mechanisms that can be used to explain most, if not all, of the observed results.

One mechanism under consideration is hydrogen trapping and trap evolution by cavity formation, caused by radiation damage and the super-saturation of hydrogen within the tungsten lattice [3–5]. The first stage of this process consists of hydrogen trapping [5,6] at impurities, dislocations, vacancies, grain boundaries, and other crystalline defects within the implantation zone. If the flux of hydrogen into the implantation zone is larger than the rate of hydrogen diffusion out of the implantation zone, all of the traps will eventually become filled, and due to the very low solubility of hydrogen in tungsten [7], there will exist a local super-saturation of mobile hydrogen. If the local effective hydrogen pressure (hydrogen fugacity) grows above a threshold value, the initial trap sites may then act as nucleation sites for multi-atomic clusters, which can grow into bubbles via dislocation loop punching [8]. This trapping mechanism will therefore be sensitive to the mobile hydrogen concentration. Since this mechanism traps multiple hydrogen atoms at the previously existing defects, it will be the dominant trap mechanism. Bubble formation due to

* Corresponding author. Tel.: +1-416 667 7868; fax: +1-416 667 7799.

E-mail address: jwdavis@starfire.utias.utoronto.ca (J.W. Davis).

0022-3115/02/$ - see front matter © 2002 Elsevier Science B.V. All rights reserved.
PII: S0022-3115(02)00946-7

hydrogen ion irradiation has been seen in tungsten [3,4,9]. This paper is a study of hydrogen retention in single crystal tungsten as a function of the incident ion flux at selected fluences.

2. Experiment

2.1. Specimens

Several mechanically and electro-polished single crystal tungsten specimens (SCW), measuring 3×6 mm and 0.4 mm thick, were provided by V.Kh. Alimov. The manufacturer, the State Institute of Rare Metals (Moscow), quoted the purity as 99.9 at.% with the main impurities being H (0.02 at.%), C (0.05 at.%) and O (0.05 at.%). High purity single crystal tungsten specimens, being almost completely free of grain boundaries and dislocations, were chosen to help reduce the number of variables that could affect D retention. Two sets of data were obtained, corresponding to slightly different specimen preparation procedures. In the *original data set*, the received specimens were annealed once at 1350 K for 10 min prior to the first implantation, with background pressures of 10^{-4} Pa during the anneal. No subsequent heat treatment or polishing was performed. For the *most recent set of data*, the specimens were mechanically polished and then electro-polished prior to each implantation, removing approximately 3–6 μm from the surface. With this polishing treatment, the previous implantation zone was removed, thus eliminating any memory or hysteresis effects [10]. The specimens corresponding to the *most recent data* also underwent a much more rigorous high temperature anneal after each polishing treatment. These specimens were annealed at 1775 K for 30 min (5 K/s heating rate, 1 K/s cooling rate), with background pressures of 10^{-5} Pa. The current temperature for the anneal is less than half the melting temperature for tungsten (3680 K), so it is unlikely that point defects or dislocations will be removed entirely with this heat treatment, especially from the bulk. However, the temperature is high enough to remove any electro-polish residue from the surface, as well as some impurities, vacancies and dislocations in the near surface that were not removed by the electro-polish, and to reduce the dislocation content in the bulk [6,11]. This more stringent technique of specimen preparation is expected to lead to a cleaner and more consistent surface in terms of both impurity content and structure.

2.2. D^+ implantation

All implantations were performed in an ultra-high vacuum accelerator facility using D_3^+ ions at normal incidence to the test specimen, without prior system bake-out. The background pressure was typically 5×10^{-5} Pa with the D_3^+ beam off, and 10^{-4} Pa during implantation. For more details of this facility, see Ref. [10]. For the most recent set of data, a liquid N_2 (LN_2) cold finger was installed in the specimen target chamber to reduce the hydrocarbon and water partial pressures and thus maintain a cleaner surface during implantation. It has been suggested that surface contamination reduces surface recombination in metals [12].

Implantations were performed using 1.5 keV D_3^+ ions (500 eV/D^+) with the flux controlled at $0.01–5.0 \times 10^{19}$ D^+/m^2 s. In order to reduce spatial beam flux variations, only the central part of the beam was allowed to impact the specimen through a 2 mm limiting aperture. An ion-energy of 500 eV/D^+ was chosen because it is below the energy threshold for creating ion damage, and thus eliminates another variable that could affect D retention. For all experiments, a 2.5 keV D_3^+ beam was utilized, with the specimen biased to +1000 V to decelerate the beam and minimize secondary electron loss. (The incident particles are designated D^+ although not all of the deuterium atoms are ionized in the D_3^+ molecular ion.) To achieve the lower fluxes, the final electro-static lens of the accelerator was defocused.

2.3. Thermal desorption spectroscopy

Thermal desorption spectroscopy (TDS) was performed in a separate vacuum system, with delays of 8–30 h between implantation and desorption. Since the diffusion coefficient at 300 K is $\sim 10^{-13}$ m^2/s (diffusion length of ~68 μm in 8 h) [6], only trapped D (no mobile D) was measured. In the *original set of data*, the TDS system was not baked and had typical base pressures of 8×10^{-6} Pa. For the most recent data, the TDS system was briefly baked (1.5 h), giving base pressures of 2.5×10^{-6} Pa after several hours of cooling. In the baked TDS system, the main background component was D_2 from a D_2 calibrated leak bottle (60%), with water constituting the secondary component (20%).

During TDS, a resistively heated W foil cradle was used for heating the implanted specimen. For the original data set, the temperature of the specimen was measured by an optical pyrometer. Temperature ramping rates during thermal desorption were 5–10 K/s. A maximum temperature of 1400 K was reached and held for 2–5 min during each TDS heating cycle. Temperature measurement for the most recent data was achieved using a 76 μm W–5%Re/W–26%Re thermocouple spot-welded onto the surface of the SCW specimen, via a platinum wire interface, after removal from the implantation chamber. This thermocouple allowed accurate temperature measurements from 300 K to >2000 K, whereas the pyrometer was susceptible to focusing and alignment errors, and was limited to a range of 600–1400 K. Temperature ramping rates during thermal desorption for the *most recent data set* were 4–6 K/s, with a

maximum temperature of 1775 K held for 5 min, and a 2 K/s post-TDS cooling rate.

The amount of D retained in the specimen was determined by integrating the quadrupole mass spectrometer (QMS) signals for D_2, HD, and D_2O (the D_2O signal was used only in the most recent data; contributions from HDO were negligible) during thermal desorption. The QMS was calibrated in situ at the start of each TDS run using a D_2 calibrated leak bottle. The relative sensitivity of H_2 to D_2 was checked periodically using H_2 and D_2 calibrated leak bottles and did not change with time. The QMS library value was used for the relative sensitivity of H_2O to H_2. Due to the size of the background D_2 leak signal, the D_2 leak bottle was closed during thermal desorption. The sensitivity to HD was assumed to be the average of the H_2 and D_2 sensitivities, and the sensitivity to D_2O was assumed to be the same as for H_2O. The acquisition of a new Hiden Analytical QMS used to obtain the *most recent data* allowed better resolution and higher sensitivity during TDS than could be achieved with the Leybold Transpector QMS used to obtain the *original set of data*. The Hiden QMS allowed the detection of a D_2O peak during thermal desorption, contributing 2–7% of the total D retained. The advantages of the Hiden QMS are reflected in the reduced uncertainty associated with each data point.

3. Results

The *original set* of flux dependence data is plotted in Fig. 1. The curves are drawn to guide the eye. A decrease in retention can be seen for the lowest fluxes, with the most noticeable drop in retention at the lower fluence used (10^{21} D^+/m^2). However, due to the large scatter in the data, we cannot draw firm conclusions for the existence of a flux dependence of D retention. The goal of the most recent experiments was to improve reproducibility of the measurements and to reduce the scatter in the data.

A thorough examination of the original set of data was performed in an effort to identify the possible sources of scatter and uncertainty. Tracing the history of each data point revealed that D retention values obtained later in the data set were generally higher than those recorded earlier. The latter results would have seen multiple implantations on the same spots since no intervening surface treatments were performed. It is highly probable that some of the scatter was due to an implantation memory or hysteresis effect, where D retention can increase as a function of the cumulative fluence on a particular spot. Such an effect was observed for polycrystalline tungsten [10]. A similar set of experiments was performed with the SCW: it was found that by the fourth implantation on the same spot, D retention was double the value obtained in the first implantation, confirming the existence of a memory effect.

The large uncertainty associated with some of the earlier data points was due to limitations of the QMS. A large signal at one mass peak would tend to overflow into adjacent masses, giving a higher apparent value for those neighbouring masses. In particular, the large H_2 peak (usually several orders of magnitude larger) tended to overlap the HD (mass 3) signal, giving a large apparent signal. Thus, the HD contribution to retention ranged anywhere from 5% to 70%, depending on the

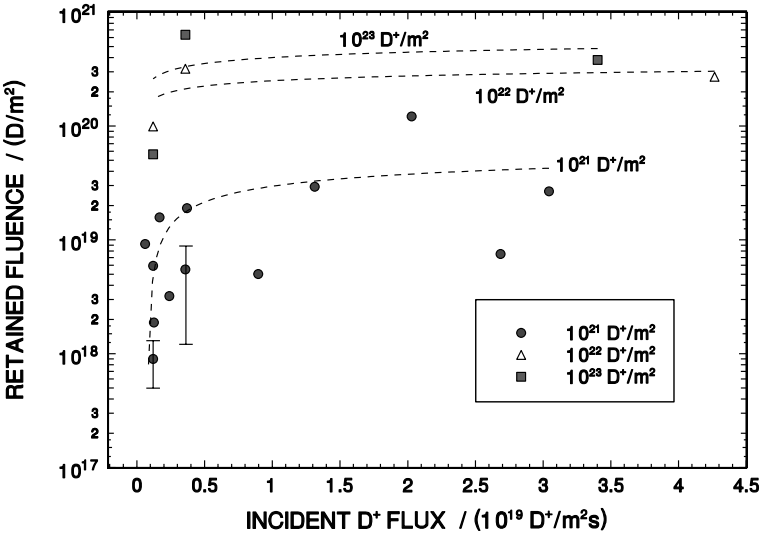

Fig. 1. Original data: deuterium retention as a function of incident D^+ flux at three fluences (10^{21}, 10^{22}, and 10^{23} D^+/m^2) at room temperature. Curves are drawn as guides only.

amount of overflow. A very large H_2 peak would even overflow into the D_2 signal. The new Hiden QMS eliminated this overflow effect. In addition, a better vacuum reduced the size of the H_2 signal.

Other possible sources of the scatter were differences in local surface conditions due to the large-scale roughness (~10 μm) of the received specimens, or differences in heating rates. Variation of the heating rate from 2 to 10 K/s was shown to have very little effect on total retention [5], although it did affect the shape of the TDS spectrum. Varying levels of surface impurities during implantation may also have contributed to the uncertainty [5,12].

The most recent data (Fig. 2) reflect the changes to reduce the scatter and to obtain more reliable, reproducible results; details of these changes were noted in the experimental section. The scatter has been reduced and the resulting uncertainty associated with each data point is estimated to be less than 10% (too small to show in this figure). The detectable limit is estimated at 5×10^{17} D/m^2, based on the ability to resolve a clean desorption peak. Again, the curves are drawn to guide the eye. A significant decrease in retention can be seen for fluxes less than 1×10^{18} D$^+$/m^2 s at a fluence of 10^{21} D$^+$/m^2. A much less prominent decrease is seen with the 10^{22} D$^+$/m^2 fluence at low fluxes. The data in Fig. 2 have also been separated into groups corresponding to different implantation or polishing conditions. The fact that the data fall into distinct groups, based solely on different surface conditions, is an indication of sensitivity to surface preparation.

4. Discussion

From both sets of data (Figs. 1 and 2), it is clear that a flux-dependence does exist. A sharp decrease in retention is seen at low fluxes for the low fluence case (10^{21} D$^+$/m^2), substantiating the hypothesis of a flux threshold mechanism. Decreases in retention at low fluxes are also seen with the higher fluence data. These results reinforce the concept of trapping via cluster/bubble formation. However, in the process of investigating the flux dependence of D retention in tungsten, it became clear that there were significant effects due to experimental procedure. As noted in Fig. 2, differences in surface conditions can give rise to significant differences in D retention. For some data (10^{21} D$^+$/m^2 fluence), the only difference was the grade of polishing paper used in the mechanical polishing treatment. When using a 1200 grit paper (Leco Corp.) on the SCW specimens, the surface was clean and shiny, but surface scratches from the paper were visible even after electro-polishing. With a 1200 *fine* grit paper (also from Leco Corp.), the surface was noticeably smoother, being largely free of visible scratches and having a brighter polished finish. The same electro-polish then followed in both cases (1 wt% NaOH, 10 V, Pt cathode, 2.5 min at room temperature). The specimens with the *fine* grit polish showed consistently lower D retention amounts at the same flux. The relatively brief electro-polish treatment may not have been able to remove all of the surface damage caused by the deeper scratches of the coarser grit paper. With an implantation depth of only 10 nm for 500 eV D$^+$ ions [13], polishing damage in the near surface

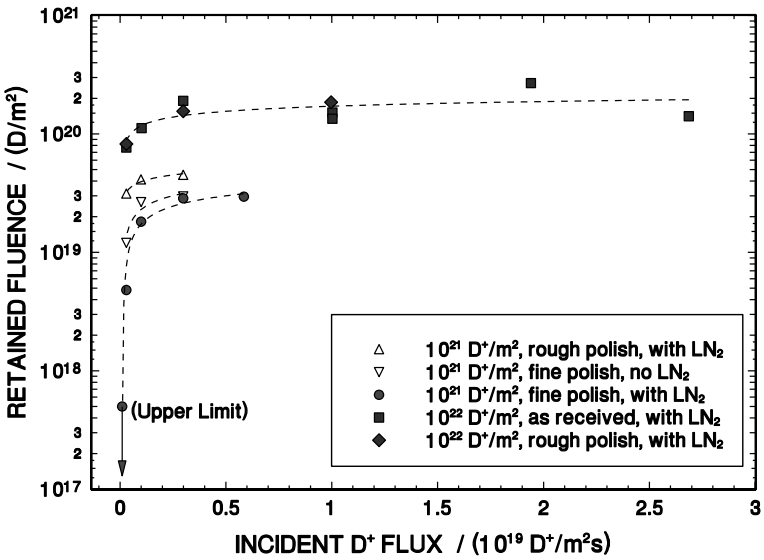

Fig. 2. Most recent data (improved experimental conditions): deuterium retention as a function of incident D$^+$ flux at fluences of 10^{21} and 10^{22} D$^+$/m^2 fluence at room temperature and various experimental conditions. Curves are drawn as guides only.

would represent an additional source of traps, leading to higher retention.

In other experiments at 10^{21} D^+/m^2, one set of specimens was implanted with LN_2 in a cold finger, while the other set was implanted without using LN_2. The implantations with the LN_2 in the cold finger consistently gave lower D retention values at the same flux. The effect of the LN_2 was to condense water vapour and heavy hydrocarbons, thereby reducing their partial pressures and surface contamination. Higher degrees of surface contamination would decrease surface recombination of hydrogen [12], leading to an increase in the mobile hydrogen concentration at the same flux, and a greater probability of cluster or bubble trapping. Even with the various changes in surface conditioning, the location of the thermal desorption peak was largely unchanged (Fig. 3). This indicates that the difference in D retention was mainly due to the amount of trapping, and not the type or energy of traps.

These cases show that D trapping is sensitive to surface conditions at low fluxes and low fluences. However, at higher fluxes or high fluences, sensitivity to surface conditions appears be much less pronounced. Comparing the retention data for the 10^{21} D^+/m^2 fluence case, with and without the LN_2 (Fig. 2), the effect of using LN_2 is most noticeable at the lowest flux, while at the higher flux of 3×10^{18} D^+/m^2 s, the effect is negligible. The partial pressure of water and hydrocarbons in the implantation chamber is estimated to be 5×10^{-5} Pa (without LN_2), and assuming a sticking coefficient of 0.5 (appropriate for a clean metal surface [12]), a flux of about 2×10^{18} D^+/m^2 s should be sufficient to maintain a clean surface. A decrease in surface recombination caused by surface contamination would decrease the minimum flux required to create the necessary hydrogen concentration for cluster/bubble trapping.

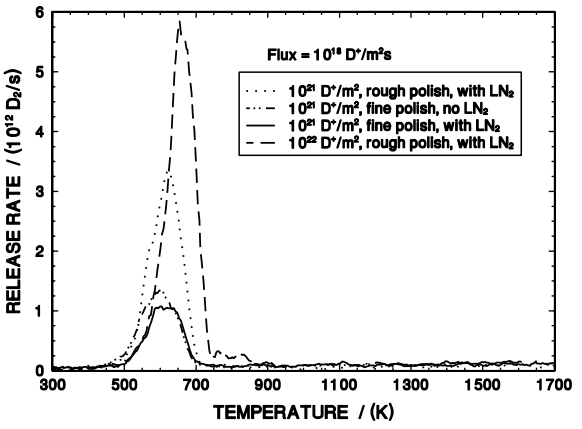

Fig. 3. Thermal desorption spectra showing the effects of different surface conditions for an incident flux of 10^{18} D^+/m^2 s. The integrated areas of these spectra are plotted in Fig. 2, above.

For the higher fluence (10^{22} D^+/m^2) experiments, the flux dependence appears to be much more subtle (Fig. 2). At higher fluences, the system will reach a steady state between the incident D^+ flux and the D diffusion flux out of the implantation zone, such that the local mobile hydrogen concentration does not change. Cluster/bubble trapping is thought to occur when the local hydrogen concentration exceeds a threshold value. If the flux is too low, there should be essentially no cluster/bubble trapping for any fluence. However, if the steady-state hydrogen concentration is sufficient for cluster/bubble trapping (above the threshold level), then for higher fluences, D retention will be largely independent of the incident ion flux. Deuterium retention at higher fluences also appears to be independent of surface conditions. This is seen in Fig. 2, as the effect of polishing, even at the lowest fluxes, is negligible for the higher fluence implant of 10^{22} D^+/m^2. It then follows that if the majority of trapping is in clusters or bubbles, *at high* D^+ *fluences*, D retention will be largely independent of surface conditions, impurity content, lattice defect concentration and flux (above the threshold). This is consistent with previous experiments where deuterium retention was seen to be essentially the same in polycrystalline W, single crystal W, and W–1%La_2O_3 at high fluence and 300 K [14,15].

5. Conclusions

Deuterium retention in single crystal tungsten was found to vary significantly at low D^+ fluxes and low D^+ fluences (10^{21} D^+/m^2). The prominent decrease in retention for fluxes below 10^{18} D^+/m^2 s suggests a flux threshold level for D retention. A smaller decrease in retention with decreasing flux was also observed at the higher fluences. The observed flux dependence of D retention in SCW is consistent with cluster/bubble trapping, brought on by a high mobile hydrogen concentration in the implantation zone. Surface conditions (polishing and contamination) were found to have a significant influence on D retention at low fluence (10^{21} D^+/m^2) and low fluxes, but negligible effects at high fluence (10^{22} D^+/m^2) or high fluxes. This observation is consistent with the hypothesis that surface impurities lead to a reduction of surface recombination of D atoms, which in turn lead to an increase of mobile D concentration in the implantation zone, and hence to a relatively higher D retention than with an impurity-free surface.

Acknowledgements

This work was supported by the Natural Sciences and Engineering Research Council of Canada and ITER Canada. We wish to thank Salvatore Boccia of the

Metals and Materials Science department, University of Toronto, for his help with specimen preparation, and V.Kh. Alimov for providing us with the high purity SCW.

References

[1] J.B. Whitley, D.A. Buchenauer, J. Nucl. Mater. 155–157 (1988) 82.
[2] R.A. Causey, T.J. Venhaus, Phys. Scr. T 94 (2001) 9.
[3] A. van Veen et al., J. Nucl. Mater. 155–157 (1988) 1113.
[4] V.Kh. Alimov, K. Ertl, J. Roth, J. Nucl. Mater. 290–293 (2001) 293.
[5] R.G. Macaulay-Newcombe, A.A. Haasz, M. Poon, J.W. Davis, in: A. Hassanein (Ed.), Hydrogen and Helium Recycling at Plasma Facing Materials, NATO Science Series II, vol. 54, Kluwer Academic, 2002, p. 145.
[6] R.A. Anderl et al., Fus. Technol. 21 (1992) 745.
[7] R. Frauenfelder, J. Vac. Sci. Technol. 6 (3) (1968) 388.
[8] J.B. Condon, T. Schober, J. Nucl. Mater. 207 (1993) 1.
[9] R. Sakamoto, T. Muroga, N. Yoshida, J. Nucl. Mater. 220–222 (1995) 819.
[10] A.A. Haasz, M. Poon, J.W. Davis, J. Nucl. Mater. 266–269 (1999) 520.
[11] H. Eleveld, A. van Veen, J. Nucl. Mater. 212–215 (1994) 1421.
[12] O.V. Ogorodnikova, J. Nucl. Mater. 290–293 (2001) 459.
[13] W. Eckstein, Computer simulation of ion-surface interactions, in: Springer Series in Material Science, vol. 10, Springer, Berlin, 1991.
[14] A.A. Haasz, J.W. Davis, M. Poon, R.G. Macaulay-Newcombe, J. Nucl. Mater. 258–263 (1998) 889.
[15] A.A. Haasz, M. Poon, R.G. Macaulay-Newcombe, J.W. Davis, J. Nucl. Mater. 290–293 (2001) 85.
[16] V.Kh. Alimov, B.M.U. Scherzer, J. Nucl. Mater. 240 (1996) 75.
[17] A.A. Pisarev, A.V. Varava, S.K. Zhdanov, J. Nucl. Mater. 220–222 (1995) 926.
[18] R. Sakamoto, T. Muroga, N. Yoshida, J. Nucl. Mater. 233–237 (1996) 776.